

Reference frame Parameter	Notes
3D or 2D motion correction	If there is little axial motion, then just 2D motion correction can be selected to minimise imaging overhead
Number of X Pixels	X dimension of reference frame
Number of Y pixels	Y dimension of reference frame
Number of Z pixels	Length of Z line scan
Size of Z pixels	Resolution of Z line scan
Number of Z scans	Number of axial scans to be averaged over
Dwell time per pixel	Can be set between 50 – 4000 ns
FOV of reference frame	FOV of Z-stack from which the reference is selected
Number of pixels in reference Z-Stack frame	Resolution of reference Z-stack
FOV of the reference Z-Stack frame	Used to ensure a reference bead is within the FOV and optimise the pixel size in the reference frame
Proportional, Integral, Differential (PID)	Default P = 0.9, I = 400, D = 0
Time between reference scans	Default 2 ms can be set 1-1000 ms
Reference channel	The channel to use for the correction (red or green in our system)

Supplementary Table 1: User defined parameters for optimising RT-3DMC

User defined parameters and options for RT-3DMC system. These enable the user to make trade-offs between imaging overhead, SNR and RT-3DMC precision using reference frame parameters for the size, resolution, dwell time and time between reference scans. The PID can be tuned to optimise performance for movements with different frequency characteristics.

General power settings: Mice ; Power to sample between 13mW and 42mW (13-18 close to the surface, then linear increase to 42 at depth of 300 or more). Fish ; Power to sample between 13mW and 18mW (13 close to the top, then linear increase to 18 at depth of 150 and more). Power on reference : Typically 15mW at the surface on beads																	
Fig.	Imaging type	Note / Experiment purpose	Example/Gro	N	Pixel	Dwell	frame rate	FOV // patch	MC	Ref	# Ref	# Ref	Z	Ref	PID	Tref	
Main text																	
Fig. 1 Hardware, Design & Performances																	
a	Patch imaging on dendrite	Example of moving tissue	example	2	0.3 ; 0.4	0.4	574 ; 429	250 // 30x9 ;	Off	N/A	N/A	N/A	N/A	N/A	N/A	N/A	
b	Z-stack	Experimental design	example	1	0.49	0.1	18	250	On	4	18x18	3	2	0.1	P=0.8/0.9,I=400	2ms	
c-e	N/A	Hardware implementation	N/A	N/A	N/A	N/A	N/A	N/A	N/A	N/A	N/A	N/A	N/A	N/A	N/A	N/A	
f	Patch imaging on dendrites/soma	Power spectrum	group data	5	1.25	400	138-190	250// 30x30	Off	N/A	N/A	N/A	N/A	N/A	N/A	N/A	
g	UDE on reference	Performance assessment	example	1	1 bead	1	500Hz	300	On	4	18x18	3	2	0.1	P=0.9,I=400	2ms	
h	piezo beads performance UDE	Performance assessment	group data	4	beads	1	500Hz	300	On	4	18x18	3	2	0.1	P=0.9,I=400	2ms	
i	piezo beads performance UDE	Performance assessment	group data	4	beads	1	500Hz	300	On	4	18x18	3	2	0.1	P=0.9,I=400	2ms	
j	piezo beads performance UDE	Performance assessment	group data	4	beads	1	500Hz	300	On	4	18x18	3	2	0.1	P=0.9,I=400	2ms	
Fig. 2 Performances in Vivo in mice																	
a	Patch imaging on dendrites/soma	MC log/UDE mouse	example	1	0.3	0.4	38	250 // 15x14	On	4	18x18	3	2	0.1	P=0.9,I=400	2ms	
b	Volume imaging on soma	Z Correction X20, group data in sup 6a	example	1	0.4	0.4	46	200 // 20x32	On/Off	4	18x18	3	2	0.1	P=0.8/0.9,I=400	2ms	
c	Patch imaging on dendrite/axon	XY correction / RT 9d-MC vs post hoc	example	1	0.2	0.4	64	250 // 100x10	On/Off	4	18x18	3	2	0.1	P=0.8,I=400	2ms	
d	Patch imaging on dendrites/soma	Sharpness improvement	group data	7	0.25-1	0.4	37-153	250/350 // 15-25	On/Off	4	18x18	3	2	0.1	P=0.8,I=400	2ms	
e	Patch imaging on dendrites/soma	Dist. UDE mouse running x20	group data	8	0.25-1	0.4	37-153	250/350 // 15-25	On/Off	4	18x18	3	2	0.1	P=0.8/0.9,I=400	2ms	
f	Patch imaging on dendrites/soma	XY UDEs mouse X20	group data	8	0.25-1	0.4	37-153	250/350 // 15-25	On/Off	4	18x18	3	2	0.1	P=0.9,I=400	2ms	
g	Patch imaging on dendrites/soma	spatial dependency XY	group data	8	0.25-1	0.4	37-153	250/350 // 15-25	On	4	18x18	3	2	0.1	P=0.8/0.9,I=400	2ms	
h	Patch imaging on dendrites/soma	spatial dependency Z	group data	8	0.25-1	0.4	37-153	250/350 // 15-25	On	4	18x18	3	2	0.1	P=0.9,I=400	2ms	
Fig. 3 Stability and photodamage																	
a	Z-stack	impact on physiology, stability, photodamage	example	1	0.59	0.1	18	300	On	4	18x18	3	2	0.1	P=0.9,I=400	2ms	
b	volume extracted from stack	impact on physiology and ref bleaching	group data	4	0.25-1	0.1	37-153	300 // 20x20x40	On	4	18x18	3	2	0.1	P=0.9,I=400	2ms	
c	Patch imaging on dendrites/soma	$\Delta F/F$ over time	example	1	0.25-1	0.4	37-153	300 // 25x25	On	4	18x18	3	2	0.1	P=0.9,I=400	2ms	
d	Patch imaging on dendrites/soma	impact on physiology ($\Delta F/F$ and freq.)	group data	4	0.25-1	0.4	37-153	300 // 25x25	On	4	18x18	3	2	0.1	P=0.9,I=400	2ms	
Fig. 4 Impact on Calcium measurements																	
a	Point imaging on soma	targetting / sample example	example	1	1	0.4	84	300 // 20x20	On	4	18x18	3	2	0.1	P=0.9,I=400	2ms	
b	Point imaging on soma	example of traces affected by movement	example	1	PSF	4	2024	300 // PSF	On/Off	4	18x18	3	2	0.1	P=0.9,I=400	2ms	
c	Point imaging on dendrite	targetting / sample example	example	1	PSF	0.4	55	300 // PSF	On	4	18x18	3	2	0.1	P=0.9,I=400	2ms	
d	Point imaging on dendrite	example of traces affected by movement	example	1	PSF	4	3318	300 // PSF	On/Off	4	18x18	3	2	0.1	P=0.9,I=400	2ms	
e	Point imaging on dendrite & soma	power spectrum on tdTomato signal	group data	4	PSF	4	2024-3420	300 // PSF	On/Off	4	18x18	3	2	0.1	P=0.9,I=400	2ms	
f	N/A	position of patches in stack	N/A	N/A	N/A	N/A	350	N/A	N/A	N/A	N/A	N/A	N/A	N/A	N/A	N/A	
g	N/A	False positive / negative sigN/AIs due to movement on small structures	N/A	N/A	N/A	N/A	200-300// 10x10	N/A	N/A	N/A	N/A	N/A	N/A	N/A	N/A	N/A	
q	HD patches on dendrites/spines	movement on small structures	example	1	0.25-1	0.4	64	250 // 25x25	On/Off	4	18x18	3	2	0.1	P=0.8,I=400	2ms	
h	HD patches on dendrites/spines	Rate of false positive events	group data	8	0.25-1	0.4	17-122	200-300// 10x10	On/Off	4	18x18	3	2	0.1	P=0.8/0.9,I=400	2ms	
Fig. 5 Performances in Vivo in Zebrafish																	
a	Z-stack	experimental design	example	1	0.68	0.1	18	350	On	4	18x18	3	2	0.1	P=0.9,I=400	2ms	
b	Patch imaging on soma	MC loss swimming	example	1	0.8	0.4	31	350 // 15x15	On	5	18x18	3	2	0.2	P=0.9,I=400	1ms	
c	Patch imaging on soma	Power spectrum	group data	5	0.5-1	0.4	116-210	350 //	Off	N/A	N/A	N/A	N/A	N/A	N/A	N/A	
d	Patch imaging on soma	XY UDEs fish X20	example	1	0.5-0.8	0.4	17-33	350 // 15x15	On	5	18x18	3	2	0.2	P=0.9,I=400	1ms	
e	Patch imaging on soma	spatial dependency with XY	group data	3	0.5-0.8	0.4	17-33	350 // 15x15	On	5	18x18	3	2	0.2	P=0.9,I=400	1ms	
f	Patch imaging on soma	spatial dependency with Z	group data	3	0.5-0.8	0.4	17-33	350 // 15x15	On	5	18x18	3	2	0.2	P=0.9,I=400	1ms	
g	Patch imaging on soma	Projection image during swimming	example	1	0.8	0.4	31	350 // 15x15	On/Off	5	18x18	3	2	0.2	P=0.9,I=400	1ms	
h	Patch imaging on soma	Dist. UDE fish X20	group data	3	0.5-0.8	0.4	17-33	350 // 15x15	On/Off	5	18x18	3	2	0.2	P=0.9,I=400	1ms	
i	Patch imaging on soma	XY UDEs fish X20	group data	3	0.5-0.8	0.4	17-33	350 // 15x15	On/Off	5	18x18	3	2	0.2	P=0.9,I=400	1ms	
Fig. 6 Impact on Calcium measurements (fish)																	
a	N/A	position of patches in stack & soma identification	example	1	0.8	N/A	N/A	350 // 15x15	N/A	N/A	N/A	N/A	N/A	N/A	N/A	N/A	
b	Patch imaging on soma	tracs MC on vs off ; Identification of artefacts	example	1	0.8	0.4	31	350 // 15x15	On/Off	5	18x18	3	2	0.2	P=0.9,I=400	1ms	
c	Patch imaging on soma	Average $\Delta F/F$ during swim	example	1	0.8	0.4	31	350 // 15x15	On/Off	5	18x18	3	2	0.2	P=0.9,I=400	1ms	
d	Patch imaging on soma	Impact on spike inference during swim	group data	3	0.5-0.8	0.4	17-33	350 // 15x15	On/Off	5	18x18	3	2	0.2	P=0.9,I=400	1ms	
e	Point imaging on soma	position of points in stack	example	N/A	N/A	N/A	N/A	350 // PSF	N/A	N/A	N/A	N/A	N/A	N/A	N/A	N/A	
f	Point imaging on soma	500 soma activity	example	1	PSF	8	22	350 // PSF	On	5	18x18	3	2	0.2	P=0.9,I=400	1ms	
g	Point imaging on soma	Average $\Delta F/F$ during swim	example	1	PSF	8	22	350 // PSF	On	5	18x18	3	2	0.2	P=0.9,I=400	1ms	
Ext. Dat																	
1 Hardware Design																	
a-b	N/A	N/A	N/A	N/A	N/A	N/A	N/A	N/A	On!	N/A	N/A	N/A	N/A	N/A	N/A	N/A	
2 FOV and Speed performances																	
a	Full frame imaging	FOV on beads in agar	example	1	0.78	0.1	25	400	Off	4	18x18	3	2	0.1	P=0.9,I=400	2ms	
b	Z-stack	FOV in vivo around virus injection site	example	1	0.78	0.1	18	400	On	4	18x18	3	2	0.1	P=0.9,I=400	2ms	
c-d	N/A	Hardware implementation	N/A	N/A	N/A	N/A	N/A	N/A	N/A	N/A	N/A	N/A	N/A	N/A	N/A	N/A	
3 Movement in other brain structures																	
a	Full frame imaging	Identification of ROI for power spectrum in cerebellum	example	1	1	0.1	110	200	Off	N/A	N/A	N/A	N/A	N/A	N/A	N/A	
b	ROIs from full frame	UDE mouse in cerebellum	example	1	1	0.1	110	200	Off	N/A	N/A	N/A	N/A	N/A	N/A	N/A	
c	ROIs from full frame	Power spectrum cerebellum	summary	1	1	0.1	110	200	Off	N/A	N/A	N/A	N/A	N/A	N/A	N/A	
d	Full frame imaging	Identification of ROI for power spectrum in V1	example	1	1	0.1	110	200	Off	N/A	N/A	N/A	N/A	N/A	N/A	N/A	
e	ROIs from full frame	UDE mouse in V1	example	1	1	0.1	110	200	Off	N/A	N/A	N/A	N/A	N/A	N/A	N/A	
f	ROIs from full frame	Power spectrum V1	summary	1	1	0.1	110	200	Off	N/A	N/A	N/A	N/A	N/A	N/A	N/A	
4 Performance with higher N/A lens																	
a	piezo beads performance	Performance assessment	group data	4	beads	1	0.4	500Hz	300	On	4	18x18	3	2	0.4	P=0.9,I=400	2ms
5 Performance of Pointing for small Z-UDE's group data																	
a-b	Point imaging on 1 μ m beads	Ability to stay on small target	group data	N/A	PSF	1	1469	300 // PSF	On/Off	4	18x18	3	1	0.2	P=0.9,I=400	2ms	
6 Z-UDE's group data																	
a	Volume imaging on soma	Z UDE running 20X	group data	5	0.5-1	0.4	33-83	200-300//25x24	On/Off	4	18x18	3	2	0.1	P=0.9,I=400	2ms	
b	Volume imaging on soma	Z UDE running 40X	group data	4	0.25-1	0.4	37-153	200 // 20x20	On/Off	4	18x18	3	2	0.1	P=0.9,I=400	2ms	
7 Effect of SNR, depth and reference																	
a	Patch imaging on dendrites/soma	SNR vs reference type	summary	4	0.25-1	0.4	37-153	300 // 25x24	On	4	18x18	3	2	0.1	P=0.9,I=400	2ms	
b	Patch imaging on dendrites/soma	SNR vs depth	summary	4	0.25-1	0.4	37-153	300 // 25x24	On	4	18x18	3	2	0.1	P=0.9,I=400	2ms	
8 Pointing mode recording on spines																	
a-b	Point imaging on spines	Point imaging on soma	example	1	PSF	4	944	150 // PSF	On/Off	4	18x18	3	2	0.1	P=0.9,I=400	2ms	
9 Movement with a different behaviour																	
a	N/A	Schematic	N/A	N/A	N/A	N/A	N/A	N/A	On!	N/A	N/A	N/A	N/A	N/A	N/A	N/A	
b	Patch imaging on soma	power spectrum	example	6	0.5-1.25	0.4	138-275	300 // 30x30 ;	Off	N/A	N/A	N/A	N/A	N/A	N/A	N/A	
c	Patch imaging on dendrite	Example of dendrite changing in Z focus X40	example	1	0.25	1	13	150 // 15x15	Off	4	18x18	3	2	0.1	P=0.9,I=400	2ms	
d	Patch imaging on dendrite	Licking/perioral movement detection pipeline	example	1	0.25	0.4	26	150 // 15x15	Off	4	18x18	3	2	0.1	P=0.9,I=400	2ms	
e	Patch imaging on dendrites/soma	Dist. XY-UDE mouse licking x20	group data	4	0.5-1.0	0.4	37-93	300 // 25x24	On/Off	4	18x18	3	2	0.1	P=0.9,I=400	2ms	
f	Patch imaging on dendrites/soma	XY UDEs mouse licking X20	group data	4	0.5-1.0	0.4	37-93	300 // 25x24	On/Off	4	18x18	3	2	0.1	P=0.9,I=400	2ms	
g	Patch imaging on dendrites/soma	Dist. XY-UDE mouse perioral mvt X20	group data	4	0.5-1.0	0.4	37-93	300 // 25x24	On/Off	4	18x18	3	2	0.1	P=0.9,I=400	2ms	
h	Patch imaging on dendrites/soma	XY UDEs mouse perioral mvt X20	group data	4	0.5-1.0	0.4	37-93	300 // 25x24	On/Off	4	18x18	3	2	0.1	P=0.9,I=400	2ms	
i	Volume imaging on soma	Dist. Z-UDE mouse licking x20	group data	4	0.5-1.0	0.4	37-93	300 // 25x24	On/Off	4	18x18	3	2	0.1	P=0.9,I=400	2ms	
j	Volume imaging on soma	Z UDEs mouse licking X20	group data	4	0.5-1.0	0.4	37-93	300 // 25x24	On/Off	4	18x18	3	2	0.1	P=0.9,I=400	2ms	
k																	

Supplementary Notes

Supplementary Note 1:

Timing of the feedback loop

A critical challenge in using closed loop real-time processing for movement correction is to achieve sufficiently fast (i.e. submillisecond) feedback times for each displacement update ($T_{feedback}$). The feedback loop consists of several sequential steps each with a characteristic time. First, interleaving of reference scans with functional acquisition needs to be synchronised. Since the reference time-out could occur at any time during an individual line scan or point scan, it was necessary to ensure that it had completed the acquisition before switching to the reference scan. This required a handshaking protocol to indicate the time at which the first reference scan record had been loaded by the AOL controller (T_{synch}). The system then ran the XY reference scan frame, lateral update and axial scans, which took time, T_{ref} , calculated the new correction (T_{offset}) and sent it over the serial link to the control system (T_{SPI}). The control system then read each record to infer the axial position and updated the next record with the corrected offset frequencies (T_{update}).

The total loop feedback time is given by:

$$T_{feedback} = T_{synch} + T_{ref} + T_{offset} + T_{SPI} + T_{update}$$

The dominant contributor to this time is imaging the reference feature T_{ref} . For a reference image of N_x by N_y pixels and N_z Z line scans, an AOD fill time T_{AOD} , lateral update time T_c (50-60 μ s) and a dwell time of T_{dwell} .

$$T_{ref} = (T_{AOD} + (T_{dwell} * N_x)) * (N_y + N_z) + T_c$$

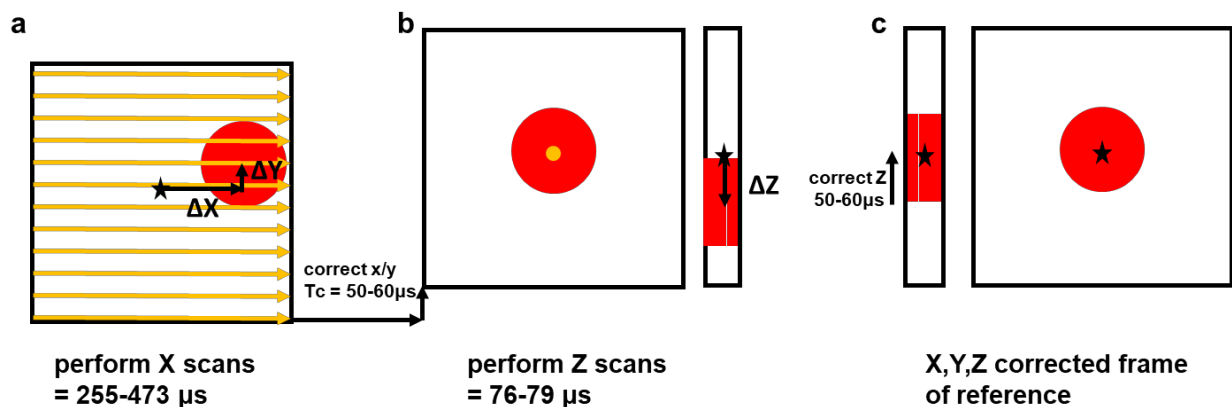
The times for each step are listed in the table below.

Feedback loop step	Time (μs)
T_{ref} (10 x 10 + 1 Z-line scan, 18 x 18 + 3 Z-line scans) $T_{dwell} = 0.1$	331 - 605
T_{synch}	56
T_{offset}	0.6
T_{SPI}	6.4
T_{update}	1
$T_{feedback}$	395-669

Supplementary Note 2:

Theoretical limits of the real time 3D movement correction

The RT 3D-MC system relies on periodically scanning a reference feature with a small XY imaging window of 10 to 18 pixels followed by 3 vertical Z-scans through the centre of the reference feature. As the reference window dynamically tracks the reference object as it moves, so the performance of the system depends on how far the reference moves between scans i.e. the maximum speed of motion. For experiments in mice we set the system to scan every 2 ms, although this is programmable to allow a trade-off between RT 3D-MC overhead and imaging time ([Supplementary Figure 2](#)). The size of the XY reference image frame imposes a limit to the maximum speed that can be corrected because the reference object must be within the reference image (Breaking Point 1).



SNFigure 1: Breaking point 1: **a:** Limit of the lateral motion that can be tracked laterally. The system first performs scans in the X direction (yellow arrows) on the bead. **b:** The lateral position is corrected and axial scans (yellow dot) are used to find the Z offset. **c:** The frame of reference is corrected in 3D (black star). Timings assume 10-18 pixels and 3 Z lines with 0.1 μ s dwell time.

For Breaking Point 1, the maximum lateral distance for accurate motion detection is $(S_x - D_b)/2$ where S_x is the reference frame size and D_b is the bead diameter in micrometers ([SNFigure 1a](#)). If the time between reference scans is T_{ref} then for Breaking point 1: $V_{max} =$

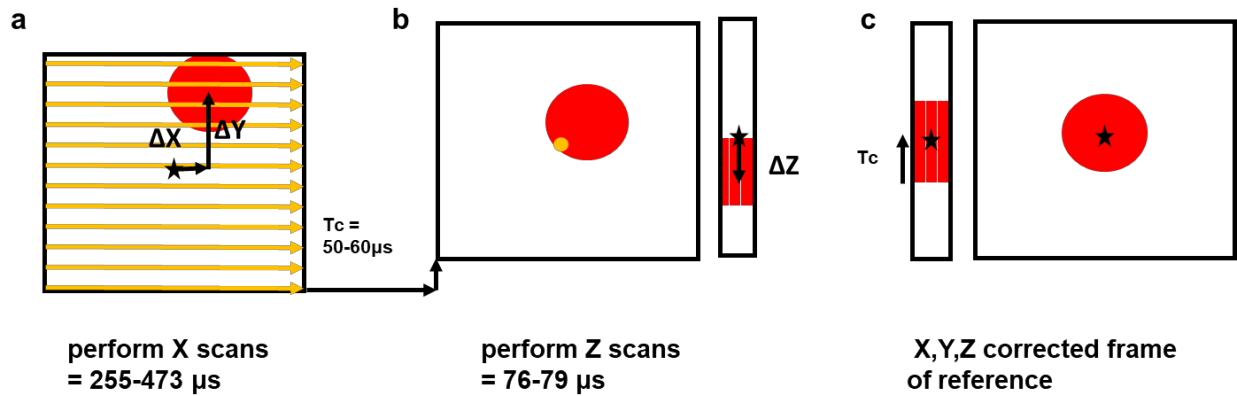
$(S_x - D_b)/(2 * T_{ref})$. With 4 μm beads, 1 μm pixels and a T_{ref} of 2 ms then $V_{max} = 1.5 \mu\text{m/ms}$ and 3.5 $\mu\text{m/ms}$ for 10 and 18 pixel windows, respectively. The following table gives the worst-case (strictest) maximum speeds in $\mu\text{m/ms}$ for Breaking Point 1.

Breaking Point 1 - max speeds ($\mu\text{m/ms}$)

T_{ref} (ms)	frame size(pixels)	Bead Diameter (μm)				
		5	4	3	2	1
2	18	3.3	3.5	3.8	4.0	4.3
1	18	6.5	7.0	7.5	8.0	8.5
2	10	1.3	1.5	1.8	2.0	2.3
1	10	2.5	3.0	3.5	4.0	4.5

SNTable 1: Breaking Point 1: Max speeds for lateral motion between reference scans

The reference object tracking system always performs a lateral adjustment before performing the Z-scans to ensure they are near the centre of the bead (**SNFigure 1a,b**). There will be an error in the centering of the Z-scans if the bead is not fully within the window as the centroid analysis will be compromised. However, for fast displacements, the time between XY scanning and adjusting for the lateral motion before performing Z scans also becomes critical. If the bead is moving fast, then the Z scans may miss the bead entirely after lateral correction (**SNFigure 2**; Breaking point 2). This is dependent on the bead size D_b , the size of the reference window ($N_x * N_y$), dwell time and update time. The worst case is when the bead is positioned at the start of the lateral scans (i.e. shifted in Y), which results in the largest delay between imaging the bead and calculating and updating its XY location for the Z scans (**SNFigure 2**). The offset update time to perform the lateral shift in the AOL controller (T_c) is equivalent to the time taken to perform 2 reference Z scans. In all our experiments the number of pixels in a Z scan $N_z = N_x$, giving a T_c of 50-60 μs .



SNFigure 2: Breaking point 2: **a:** off-center bead at the beginning of the reference scan means that for all scans after the bead, the reference may be moving undetected, **b:** Limit of lateral motion that can be tolerated between lateral and Z scans (yellow dot), **c:** The system will correct in Z as long as the scans go through the bead, but loses precision due to poorer SNR near the edge. Timings assume 10-18 pixels and 3 Z lines with 0.1 μs dwell time.

For Breaking point 2 the maximum speed tolerated by the system is $D_b / (2 * T_{fin})$, where the lateral update time (T_{fin}) to finish the frame from the last bead scan and update the controller:

$T_{fin} = (N_y - N_b) * (24.5 + N_x * T_{dwell}) + T_c$. Where 24.5 μs is the AOD fill time, T_{dwell} is the pixel dwell time and N_b is the number of scans on the bead (so $N_b = D_b$ for 1 μm reference pixels used in **SNTable 2**).

The following table gives the maximum speeds (μm/ms) for Breaking Point 2 depending on bead size, frame size and pixel dwell time.

Breaking Point 2 - max speeds (μm/ms)

T_{dwell} (μs)	frame size(pixels)	Bead Diameter (μm)				
		5	4	3	2	1
0.1	18	6.3	4.8	3.4	2.1	1.0
0.2	18	5.9	4.4	3.1	2.0	0.9
0.1	10	14.0	9.8	6.5	3.9	1.8
0.2	10	13.5	9.4	6.3	3.8	1.7

SNTable 2: Breaking point 2 speeds (μm/ms) – for missing Z scans

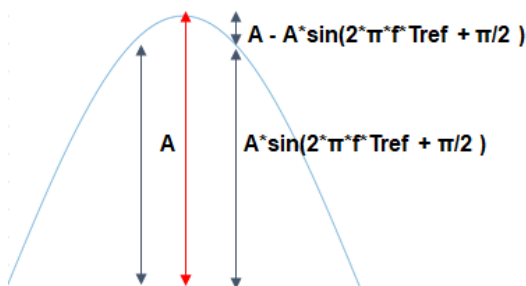
For the mouse experiments we used 4 μm beads with a dwell time of 0.1 μs , a frame size of 18x18 for the reference image and 2 ms time between reference scans, so the critical breaking speed was dependent on Breaking point 1 (3.5 $\mu\text{m}/\text{ms}$). The maximum brain speed of motion observed in mice was 0.32 $\mu\text{m}/\text{ms}$ for locomotion and 0.54 $\mu\text{m}/\text{ms}$ for licking bouts and indeed, we found 3D-MC was robust for all mouse experiments.

For zebrafish we used 5 μm beads with an 18 x 18 window with 0.2 μs dwell times and we reduced the time between reference scans to 1 ms. For zebrafish breaking point 1 occurs at 6.5 $\mu\text{m}/\text{ms}$ and breaking point 2 occurs at 5.9 $\mu\text{m}/\text{ms}$. For zebrafish the mean maximum speed was 3.6 ± 2.3 $\mu\text{m}/\text{ms}$ and the maximum speed ever observed was 7.2 $\mu\text{m}/\text{ms}$ which explains why the tracking is occasionally lost with very large, fast brain motions.

For Z motion the breaking point is due to the bead moving outside the Z scans. i.e. the same as for Breaking Point 1 in Table 1, but using the length of Z -scan rather than the frame size.

Sinusoidal Oscillations:

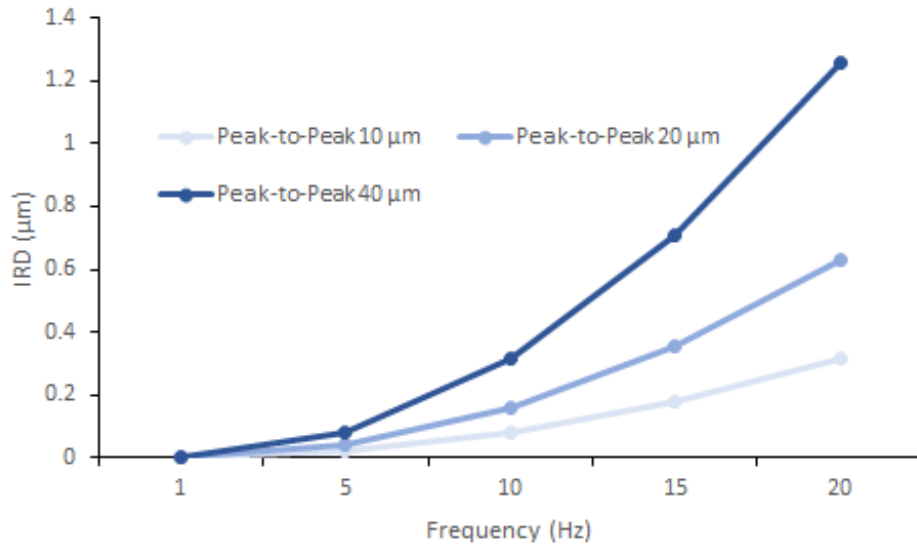
Predicting the breaking points for sinusoidal oscillations, conducted to evaluate the RT 3D-MC performance, is complicated by the variable speed and direction of motion for sinusoidal motion. For example, at the peak of oscillations, the RT 3D-MC system will correct in the wrong direction as it cannot anticipate the change in direction of motion (**SNFigure 3**).



SNFigure 3: Worst case Intercycle Reference Displacement at the peaks of sinusoidal oscillations A = Amplitude, f = frequency and T_{ref} = time between reference scans.

When the reference is read at the peak of the sinusoid (red arrow) , its sees a shift from the previous point (left black arrow) of $+1 * A * (1 - \sin(2 * \pi * f * T_{ref} + \pi/2))$ and will try and correct it. However the bead will have actually moved to $-1 * A * (1 - \sin(2 * \pi * f * T_{ref} + \pi/2))$. This gives a worst-case Intercycle Reference Displacement (IRD) at peaks given by:

$$IRD = 2 * A * (1 - \sin(2 * \pi * f * T_{ref} + \pi/2)). \quad (\text{eq.}: 1)$$



SNFigure 4: Predicted Intercycle Reference Displacement (IRD) for peak overshoots with frequency and amplitude of oscillation.

The predicted IRD (**SNFigure 4**) matches closely to the XY measured performance with oscillating beads, (**Main Figure 1h,i** and **Supplementary Figure 4**).

For sinusoidal motion, taking into account the frequency dependent tracking error at peaks, the breaking point 1 frequency is given by solving the following for f_{max} .

$$(S_x - D_b)/2 - IRD_{max} = A * \sin(2\pi * f_{max} * T_{ref}) \quad (\text{eq.}: 2)$$

where:

$$IRD_{max} = 2 * A * (1 - \sin(2 * \pi * f_{max} * T_{ref} + \pi/2)) \quad (\text{eq.}: 3)$$

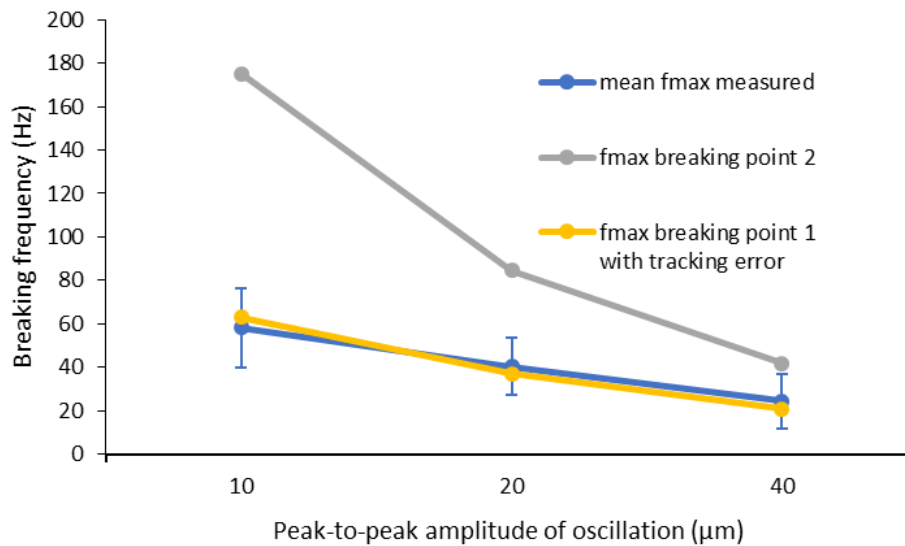
Substituting for IRD_{max} into eq. 2 and solving for f_{max} gives:

$$f_{max} = (\text{ARCSIN}(((S_x - D_b)/2 - 2*A)/(\text{SQRT}(5)*A) + \phi)) / (2*\pi*T_{ref}) \quad (\text{eq.: } 4)$$

where

$$\sin(\phi) = 2*\sin(3 * \pi / 2) \text{ determined modulo } 2*\pi.$$

We measured the breaking frequency of tracking beads, oscillating on a piezoelectric stage (with peak-to-peak oscillations of 10, 20 and 40 μm) and with reference updates every T_{ref} (= 2 ms) using 5 different 5 μm (D_b) bead reference objects.



SNFigure 5: Predicted breaking points for breaking point 2 (grey) and breaking point 1 with tracking error (yellow) and the observed breaking point blue ($n = 5$ reference beads, error bars show standard deviation).

SNFigure 5 shows the predicted breaking points for breaking point 1 (yellow), breaking point 2 (grey) and the observed breaking points across a range of peak-to-peak amplitudes (blue). For continuous sinusoidal oscillations, predicted IRDs with breaking point 1 gives a very good prediction of the observed breaking points across a range of amplitudes.

Supplementary Note 3:

Integration of an AOL 3D scanner into existing two-photon microscopes

RT-3DMC relies on the agility of the inertia-free AOL 3D scanner to perform random access scanning anywhere within the 3D FOV at 20-40 kHz. The simplest way to incorporate this technique into existing galvanometer-based systems, is to couple an AOL 3D scanner in series with a set of conventional galvanometers. By keeping the galvanometers fixed, so that they point to the centre of the field of view, the RT-3DMC functionality and 3D imaging over the 400x400x400 μm AOL imaging volume can be achieved. This dissemination solution has the advantage that it should work for most two-photon microscope setups, transforms them into high speed 3D imaging systems and will have a RT-3DMC performance that is comparable to the data presented here.

Optical path: The ~25% transmission efficiency of an AOL in series with galvanometers requires a 2W femtosecond laser. A pre-chirper is also required to introduce a $-29,000 \text{ fs}^2$ group velocity dispersion in order to compensate for chromatic dispersion through the system. The acoustic waves traveling across the AOL must be refreshed between each point or line scan. A Pockels cell or an acousto optic modulator can be used to blank the laser during this AOD fill time. Before entering the AOL the laser beam must be expanded to a 15 mm aperture with a beam expander. Telecentric optical relays are required to relay the 3D scanned output of the AOL to the galvanometer mirrors

AOL Controller: A custom-designed FPGA AOL control system was developed using a Xilinx VC707 board connected to a custom DAC board. FPGA object code and DAC-board schematics will be made available on the SilverLab repository on GitHub.

Data Acquisition: Many galvanometer systems already have high speed acquisition systems that can be reused. Specifications of our DAQ system are given in the Methods. FPGA

object code for the DAQ FPGA board will be made available on the SilverLab repository on GitHub.

Host Software: We have developed MatLab and a LabVIEW based 3D imaging software, the latest versions of which support RT-3DMC. Once an AOL scanner is added to a microscope, using either of these applications is the simplest way to get 3D imaging and RT-3DMC running. To integrate AOL scanning and RT-3DMC into other software we have also developed an Application Programming Interface (API) library for the Windows platform. The latest versions of these applications will be made available on the SilverLab repository on GitHub (See URL in Code Availability section). More detailed instructions for the integration and alignment of the AOL can be found at:

<https://github.com/SilverLabUCL/SilverLab-Microscope>

Supplementary Note 4:

Calibration

There are two main sources of distortions of the imaging volume of the AOL 3D microscope that may need to be corrected.

- (1) A tilted 3D FOV due to a slightly off-centred beam entering into the back aperture of the objective.
- (2) Changes in axial magnification due to imperfect telecentric coupling of the AOL to the microscope.

These field distortions are small but, when imaging subcellular features, need to be corrected. We have a semi-automated calibration protocol that measures the tilt and magnification distortion in the 3D FOV. These aberrations can be corrected by adjusting the acoustic drives to realign the scanned Z axis with the true Z axis (which is determined by the mechanically shifting the objective focus), and also correct for different magnification at different axial positions. After correction the drives produce a non-distorted, axially aligned 3D FOV.

The same correction parameters are also used to accurately correct for the motion tracking within the 3D FOV. The changes are calculated per scan as they vary depending on the position in the 3D FOV, imaging speed and imaging wavelength. We found this calibration correction was necessary for accurate sub-micron tracking throughout the 3D imaging volume. This was especially critical when translating the motion of the reference object (typically measured near the surface of the brain) to correct for ROIs that were distant from the reference feature.